

The Dynamin-Related Protein Mgm1p Assembles into Oligomers and Hydrolyzes GTP To Function in Mitochondrial Membrane Fusion[†]

Gabriela Meglei and G. Angus McQuibban*

Department of Biochemistry, University of Toronto, Toronto, Ontario M5S 1A8, Canada

Received September 9, 2008; Revised Manuscript Received January 9, 2009

ABSTRACT: Mitochondrial dynamics resulting from competing membrane fusion and fission reactions are required for normal cellular function in eukaryotes. Mgm1p, a dynamin-related protein, is a key component in yeast mitochondrial fusion and is evolutionarily conserved. Previous studies suggest that Mgm1p mediates mitochondrial inner membrane fusion in a manner similar to that of other dynamin proteins that use GTP hydrolysis and oligomerization to induce structural changes in lipid bilayers; however, a direct demonstration of these activities has yet to be presented. Here we show that purified Mgm1p forms low-order oligomers that are dependent on protein concentration, suggesting a dynamic and reversible interaction. We further demonstrate that Mgm1p has GTPase activity and kinetic properties consistent with a mechanoenzyme and with a role in inner membrane mitochondrial fusion. Mutations of key residues in conserved motifs of the GTPase domain show markedly reduced or diminished GTPase activity. A mutation in the GTPase effector domain, involved in assembly and assembly-stimulated GTP hydrolysis, has basal GTPase activity similar to that of wild-type Mgm1p but has a weaker propensity to form oligomers. Finally, our data indicate that Mgm1p interacts specifically with negatively charged phospholipids found in mitochondrial membranes, and point mutations in the predicted lipid-binding domain abrogate these interactions. These findings suggest the presence of a putative lipid-binding domain, providing insight into how this protein mediates inner membrane fusion. Together, these data indicate that Mgm1p mediates fusion through oligomerization, GTP hydrolysis, and lipid binding in a manner similar to those of other dynamin mechanoenzymes.

Mitochondria are dynamic organelles constantly undergoing competing fusion and fission events. The precise requirement for these dynamics is currently unknown; however, they result in the sharing of mitochondrial DNA and intracellular distribution of the mitochondrial network (1). In addition to these primary functions, mitochondrial dynamics are involved in fundamental cellular processes such as apoptosis and differentiation and have physiological consequences in embryonic development and neurodegenerative diseases (2). At the core of these processes are the molecular machines that mediate fusion and fission, a group of highly conserved GTPases belonging to the family of dynamin-related proteins (DRPs).¹ The key components in yeast mitochondrial fusion have been identified as the outer membrane spanning fuzzy onions, Fzo1p [mitofusin 1 and 2 (Mfn1 and Mfn2, respectively) in mammals], the inner membrane-associated mito-

chondrial genome maintenance protein, Mgm1p (optic atrophy OPA1 in mammals), and the fungal-specific outer membrane spanning protein Ugo1p. These proteins form a complex that mediates mitochondrial outer and inner membrane fusion in eukaryotes. Mutations in the human counterparts of Fzo1p and Mgm1p, both members of the family of DRPs, cause Charcot-Marie-Tooth-neuropathy type 2A and autosomal dominant optic atrophy, respectively, underscoring the fundamental importance of mitochondrial fusion and DRPs to the health of the cell and organism (3, 4).

Mgm1p was first identified in a screen for genes required for mitochondrial genome maintenance in yeast by Jones and Fangman and by sequence homology is a DRP (5). The domain architecture of Mgm1p starting at the N-terminus includes a mitochondrial targeting sequence (MTS), two consecutive hydrophobic segments, and the three domains common to DRPs: a GTPase, middle, and GTPase effector domain (GED) (1, 5–8). The GTPase domain and GED of Mgm1p are most highly conserved, while the middle region of the protein is more divergent. Classical dynamins contain two additional domains. The plextrin homology (PH) domain is sandwiched between the middle domain and GED and interacts with negatively charged phospholipids, and the proline-rich domain (PRD) found at the C-terminus mediates protein–protein interactions (5). There is no indication that the PRD exists in other dynamin superfamily members besides classical dynamins such as dynamin 1. However, although sequence homology cannot identify a bona fide PH

[†] G.M. was supported by an NSERC studentship, and G.A.M. is a New Investigator of the CIHR and funded by an operating grant (303157) from the CIHR.

* To whom correspondence should be addressed: 1 King's College Circle, Medical Sciences Building, Toronto, Ontario M5S 1A8, Canada. Phone: (416) 978-6820. Fax: (416) 978-8548. E-mail: angus.mcquibban@utoronto.ca.

¹ Abbreviations: ADL2, Arabadopsis dynamin-like 2; CD, circular dichroism; DRP, dynamin-related protein; DTT, dithiothreitol; Fzo1p, fuzzy onions 1 protein; GED, GTPase effector domain; Mfn1/2, mitofusin 1 and 2; Mgm1p, mitochondrial genome maintenance protein; *M_r*, relative molecular weight; MTS, mitochondrial targeting sequence; OPA1, optic atrophy 1; PH, plextrin homology; PRD, proline-rich domain; Rbd1p, rhomboid 1 protein.

domain in the DRPs, there is evidence that a lipid-binding module may exist. For instance, the DRPs Arabadobsis dynamin-like 2 (ADL2), dynamin-related protein, Dnm1p, and interferon-inducible, MxA, have all been shown to bind to lipids (9, 10). The self-assembly properties of dynamins are an important characteristic of this protein superfamily. Under nonassembly conditions (i.e., high ionic strength), dynamins form low-order oligomers such as dimers, trimers, and tetramers (11–14) that have a basal GTPase activity. Assembly of these basic oligomers into polymers of rings and helices, induced most commonly by a low ionic strength, results in a stimulated rate of GTP hydrolysis.

In yeast, Mgm1p exists in the mitochondria in two forms both required in equal proportions for proper mitochondrial morphology (6, 15). The N-terminal MTS of Mgm1p targets the preprotein to the inner mitochondrial membrane translocase, Tim23p, which pulls the peptide through until the first hydrophobic segment is reached (6). l-Mgm1p results from cleavage of the MTS by the mitochondrial processing peptidase and remains tethered to the inner membrane via the first hydrophobic segment, exposing the DRP domains to the intermembrane space (6). Alternatively, ATP-driven import through the translocase bypasses the first hydrophobic segment and embeds the second hydrophobic segment, containing a rhomboid (Rbd1p) processing site, into the inner membrane (6, 16). A cleavage event by the inner membrane serine protease, Rbd1p, releases s-Mgm1p into the intermembrane space where it remains closely associated with the inner membrane (6, 16). It has been proposed that this mechanism of regulated proteolysis links mitochondrial fusion to the energetic status of the cell.

In vitro fusion assays using yeast mitochondria have determined that outer membrane and inner membrane fusion are separable events (17). Outer membrane fusion is mediated by Fzo1p tethering and requires low levels of GTP and an inner membrane proton gradient (17). Inner membrane fusion requires Mgm1p, high levels of GTP (0.5 mM), and an inner membrane potential (17, 18). The role of Mgm1p in inner membrane fusion likely involves separable tethering and fusion steps and also appears to require the ability to self-interact in *cis* and *trans*, and a functional GTPase domain and GED (7, 18). However, the molecular mechanism by which Mgm1p mediates this process has not been determined. Mgm1p and its human homologue, OPA1, have also been shown to localize along cristae folds and at cristae junctions and to play a role in the maintenance of these structures and the release of cytochrome *c* in a manner reliant on homo-oligomerization (17, 19–23).

Despite the many lines of evidence indicating Mgm1p functions in a manner similar to that of dynamins to mediate inner membrane fusion and cristae maintenance, the activities attributed to this protein have not been directly demonstrated. Therefore, we have taken an in vitro approach to biochemically characterize Mgm1p to understand how this protein performs the diverse roles that have been ascribed to it. In this work, we demonstrate that recombinant Mgm1p is able to self-assemble and hydrolyze GTP in a manner consistent with other dynamin proteins and with a role contributing to the inner membrane dynamics of the mitochondrion as a mechanoenzyme. We also present evidence that Mgm1p is able to associate with specific negatively charged phospholipids and that mutations in the predicted PH domain abrogate

these interactions, suggesting that Mgm1p contains a novel lipid-binding module. Together, these studies provide a direct demonstration of the activities of Mgm1p and contribute to an understanding of the role of this protein in mitochondrial fusion and cristae maintenance.

MATERIALS AND METHODS

Expression and Purification of Recombinant s-Mgm1p. s-Mgm1p was amplified by PCR with the following forward and reverse primers (5'-ATACATATGGCTACTCTAAT-AGCCGCT-3' and 5'-CCTGAGCTCGCTAAATTTTGTG-GAGACGCC-3', respectively) and cloned into the pET-21(+)-b expression vector (Novagen) using *Nde*I and *Sac*I restriction sites. The construct with a C-terminal His₆ tag was transformed into *Escherichia coli* Rosetta-gami B cells (Novagen) for expression. Typically, 8 L of culture was grown at 37 °C to an optical density of 0.3, and cultures were cooled to 15 °C on ice, induced with 50 μ M IPTG, and grown for 16 h at 15 °C. Cells were harvested and lysed with a French press, and protein was purified using Ni²⁺-NTA Superflow resin (Qiagen) according to the manufacturer's specifications. Fractions were tested by SDS-PAGE, and purified protein was exchanged into 25 mM HEPES, 25 mM PIPES, 500 mM NaCl, 1 mM dithiothreitol, pH 7.5 buffer (HP500) and concentrated prior to gel filtration chromatography. Point mutations were created by the Quick Change method. Protein concentrations were measured by the Bradford assay. Protein was stored in 25% glycerol at –20 °C.

Circular Dichroism. CD measurements were obtained using a Jasco J-810 instrument in 50 mM phosphate buffer (pH 7.5), 500 mM NaCl, and 1 mM dithiothreitol at the indicated protein concentration. Protein was allowed to equilibrate for 5 min at each temperature prior to the ellipticity (millidegrees) being measured between 250 and 200 nm. Buffer alone was also measured and subtracted from the protein sample. Values for mean residue ellipticity (θ_{mr} , in deg cm² dmol^{–1}) at each wavelength were obtained by the following formula:

$$\theta_{mr} = \theta_{deg} M (c l n_r)^{-1} \quad (1)$$

where θ_{deg} is the ellipticity (degrees), M is the molecular weight of the protein (grams per decimole), c is the protein concentration (grams per cubic centimeter), l is the path length (centimeters), and n_r is the number of residues in the protein.

Gel Filtration Chromatography. All gel filtration chromatography was performed on the Superdex 200 HR 10/30 column (Amersham) in HP500 buffer unless otherwise noted. The column was calibrated with blue dextran, thyroglobulin (669 kDa), apoferritin (443 kDa), β -amylase (200 kDa), alcohol dehydrogenase (150 kDa), BSA (66 kDa), carbonic anhydrase (29 kDa), and cytochrome *c* (12.4 kDa); 250 μ L of protein was injected at a flow rate of 0.5 mL/min, and 250 μ L fractions were collected.

Cross-Linking with Glutaraldehyde. Cross-linking was conducted with glutaraldehyde at a final concentration of 0.025% in HP500 buffer with 10% glycerol and 0.5% NP-40. The protein concentration was 0.6 mg/mL. The cross-linking reaction was conducted at 4 °C for varying amounts of time before being quenched with 10 \times quenching solution

[1 M Tris and 1 M glycine (pH 7.5)] and separated by SDS-PAGE.

GTPase Activity. GTP hydrolysis activity was measured in HP500 buffer using the Malachite Green assay for inorganic phosphate determination as previously described (24). All gel filtration fractions were assayed at 1 mM GTP. Protein concentrations ranged from 0.5 to 12 μ M. Typically, 50 μ L of protein was added to 150 μ L of reaction mix containing HP500 buffer, 5 mM $MgCl_2$, 7 mM KCl, and varying amounts of GTP and incubated at 30 °C. Aliquots (20 μ L) were removed at different time points and reactions quenched with 5 μ L of 0.5 M EDTA prior to the addition of 150 μ L of a Malachite Green solution (24). The color was allowed to develop for 1 min and quenched with 25 μ L of 34% citric acid prior to measurement of the absorbance at 650 nm. A standard curve with 0–100 μ M inorganic phosphate was used to convert absorbance measurements into inorganic phosphate concentrations. All assays were conducted in 96-well plate format using a Molecular Devices plate reader.

Lipid Overlay Assay. The lipid overlay assay was conducted as previously described (25). Briefly, 1 μ L of lipid solutions ranging from 500 to 16 μ M was spotted onto nitrocellulose and incubated with 10 nM s-Mgm1p. Lipid–protein binding was detected with anti-(His)₆ antibodies and enhanced chemiluminescence.

RESULTS

Expression and Purification of Recombinant s-Mgm1p. The two functional forms of Mgm1p, long (l) and short (s), are both required in an approximately equal ratio for normal mitochondrial morphology and contain all the predicted biochemically active domains of the protein (6, 15) (Figure 1A). To understand the precise molecular role of this protein, we expressed and purified soluble recombinant s-Mgm1p to characterize its potential *in vitro* biochemical activities. Purified protein fractions from Ni^{2+} affinity chromatography were analyzed by SDS-PAGE and stained with Coomassie Brilliant Blue (Figure 1B,C). The 86 kDa band (calculated molecular mass of s-Mgm1p with the linker and His₆ tag) is >90% pure as judged by densitometry. This preparation was used to study the oligomeric state of s-Mgm1p and was further purified by gel filtration chromatography prior to GTPase activity measurements. The CD spectrum after both purification steps shows two minima at 208 and 222 nm that disappear in a cooperative manner after thermal denaturation, indicating recombinant Mgm1p is folded (Figure 1D,E).

Determination of the Oligomeric State of s-Mgm1p in 500 mM NaCl. Mgm1p is classified as a dynamin-related protein (DRP) by sequence homology and contains three of the five domains common to this family of proteins (Figure 1A). Classical dynamin proteins have been shown to form dimers and tetramers in solution under nonassembly conditions such as high ionic strength; these oligomers form the building blocks for assembly into rings and helical stacks of rings at low ionic strengths and in the presence of GTP analogues or liposomes (5). It has also been previously reported that dithiothreitol (DTT) is required for dynamins to remain stable in solution and that the absence of DTT renders these proteins inactive (24). We investigated the oligomeric state of s-Mgm1p in nonassembly (high ionic strength, 500 mM

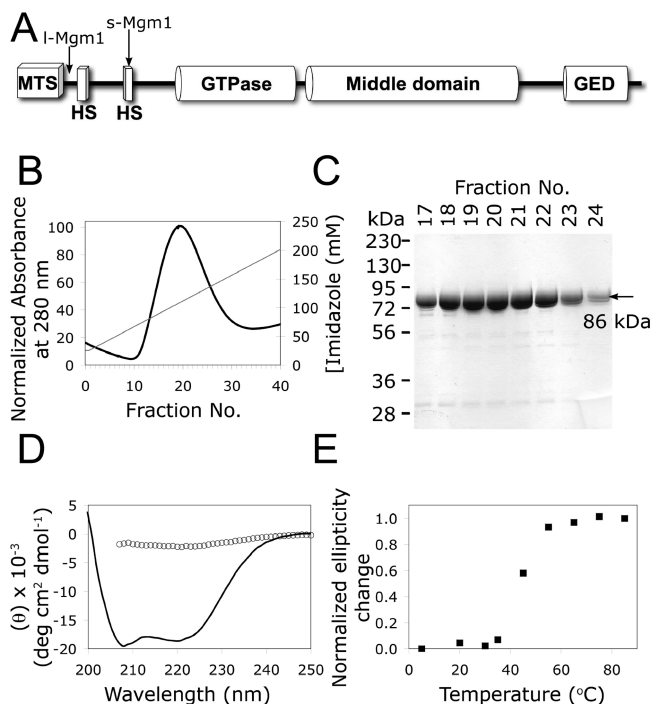


FIGURE 1: Purification and characterization of s-Mgm1p. (A) Domain schematic of Mgm1p depicting the mitochondrial targeting sequence (MTS), hydrophobic segments (HS), GTPase domain, middle domain, and GTPase effector domain (GED). The two proteolytic cleavage sites resulting in the two functional forms of the protein, long Mgm1p (l-Mgm1p) and short Mgm1p (s-Mgm1p), are marked by arrows. (B) Elution profile of s-Mgm1p from Ni^{2+} affinity resin with an imidazole gradient: (black line) absorbance at 280 nm and (gray line) imidazole concentration in millimolar. (C) SDS-PAGE of fractions collected from the imidazole elution shown in panel B. The arrow indicates the position of the 86 kDa s-Mgm1p protein (amino acids 161–902 with the linker and His₆ tag). (D) CD spectra of s-Mgm1p expressed as mean residue ellipticity at 5 °C (—) and 85 °C (○). (E) Thermal denaturation of s-Mgm1p monitored by circular dichroism at 208 nm. CD experiments were performed with 2.8 μ M s-Mgm1p in 50 mM phosphate (pH 7.5), 500 mM NaCl, and 1 mM dithiothreitol.

NaCl), reducing conditions by gel filtration chromatography and chemical cross-linking with glutaraldehyde (Figure 2). Two characteristic peaks were observed; the minor peak, *a*, has approximately 10% of the intensity of the major peak, *b* (Figure 2A,B). Both peaks have apparent relative molecular weights (M_r) that are significantly greater than that of monomeric s-Mgm1p. Specifically, the M_r of peak *a* is ~390 kDa, corresponding to approximately five monomer subunits, and the M_r for peak *b* is ~250 kDa, corresponding to approximately three monomer subunits. However, due to the shape assumptions inherent to gel filtration chromatography, these values do not necessarily reflect the actual stoichiometry of oligomers in solution. Cross-linking of the major peak resulted in the predominant formation of trimers with some higher oligomers and dimers (Figure 2C). Together, these data demonstrate that Mgm1p is able to form low-order oligomers in solution under nonassembly conditions. To further understand the presence of the minor and major peaks of s-Mgm1p under nonassembly conditions, we performed additional gel filtration studies on s-Mgm1p.

The Oligomeric State of s-Mgm1p Depends on Protein Concentration. The minor and major peaks observed by gel filtration chromatography can be a result of either of two scenarios. First, peaks that shift with protein concentration,

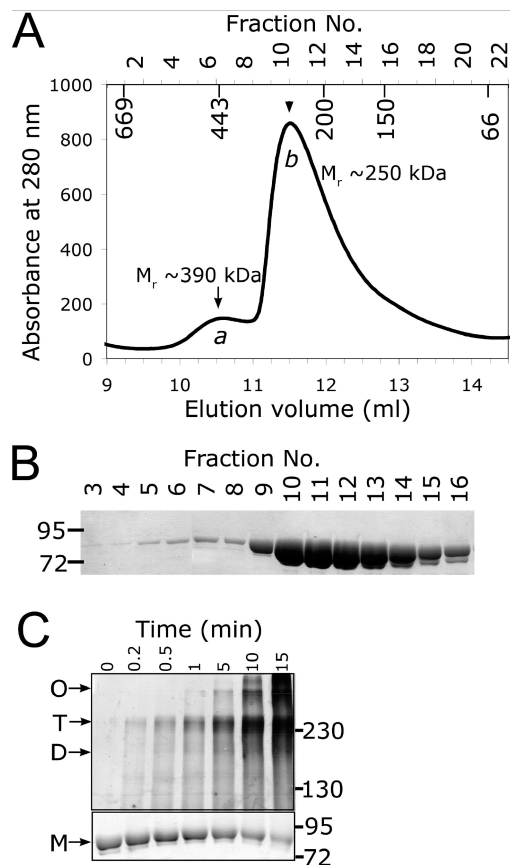


FIGURE 2: Oligomeric state of sMgm1p under nonassembly conditions. (A) Characteristic Superdex 200 gel filtration chromatogram for s-Mgm1p (20 mg/mL) depicting the minor peak (arrow, *a*) and the major peak (arrowhead, *b*). The apparent relative molecular weights (M_r) of peaks *a* and *b* are ~ 390 and ~ 250 kDa, respectively. Molecular weight markers are shown on the top x-axis inside the graph. (B) SDS-PAGE of gel filtration fractions collected in panel A. (C) Major peak s-Mgm1p cross-linked for varying times. The bottom panel is a Coomassie Blue-stained gel showing the disappearance of monomer (M). The top panel is a silver-stained gel showing the predominant formation of trimers (T). Larger oligomers (O) and some dimers (D) were also detected. All cross-linking was performed with 0.6 mg/mL protein and 0.025% glutaraldehyde at 4 °C.

are asymmetrical, and show spreading at the trailing boundary result from a self-associating solute that is rapidly and reversibly interconverting (26). Second, peaks that do not shift with protein concentration result from a nonreversible interaction or a self-associating solute in slow equilibrium (26). To determine the types of interactions s-Mgm1p forms, we conducted gel filtration experiments at four different protein concentrations (Figure 3A and Table 1). Although the apparent relative molecular weight values obtained by gel filtration cannot be used to deduce the exact stoichiometry of oligomers due to shape assumptions, they are useful for determining whether the oligomer size increases as a function of protein concentration. The apparent relative molecular weight of the minor peak remained constant at all concentrations assayed, implying this oligomer results from a slowly equilibrating or nonreversible association. However, the major peak showed a protein concentration-dependent shift in apparent relative molecular weight ranging from ~ 170 to ~ 250 kDa. Further, the peak shapes were broad and nonsymmetrical with tails at the trailing boundaries. Together, these observations indicate the self-association of

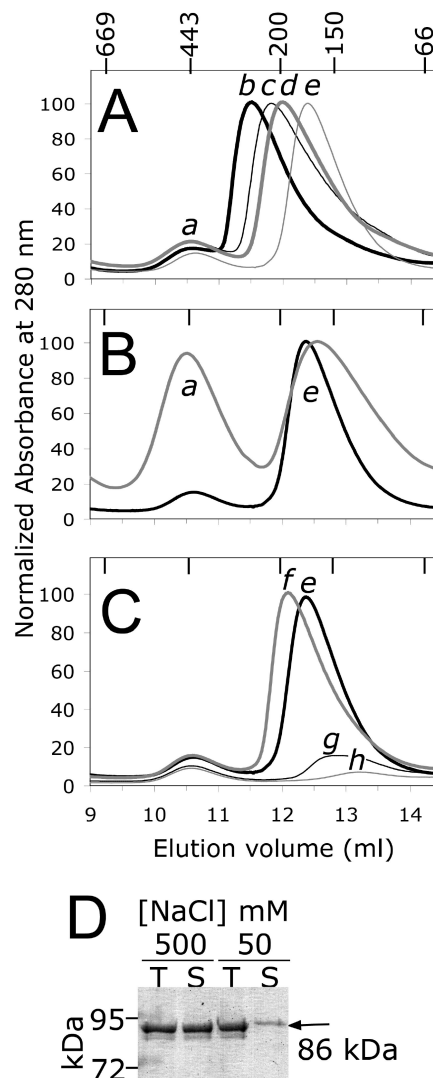


FIGURE 3: Oligomeric state of s-Mgm1p under different conditions. (A) Oligomeric state of s-Mgm1p at different protein concentrations: 20 mg/mL (thick black line), 17 mg/mL (thin black line), 11 mg/mL (thick gray line), and 2 mg/mL (thin gray line). Apparent relative molecular weights of peaks *a*, *b*, *c*, *d*, and *e* are 390, 250, 220, 200, and 170 kDa, respectively (see Table 1). Molecular mass markers are shown on the top x-axis, and the y-axis was normalized to 100 for each concentration. (B) Oligomeric state of s-Mgm1p in the absence (gray line) and presence (black line) of dithiothreitol. The y-axis was normalized to 100 for both conditions. (C) Oligomeric state of s-Mgm1p at different NaCl concentrations. A 20 mg/mL stock solution of s-Mgm1p in HP500 buffer was diluted 10-fold into similar buffers containing 500 mM (thick black line), 300 mM (thick gray line), 150 mM (thin black line), and 50 mM NaCl (thin gray line) and allowed to equilibrate for 24 h at 4 °C. The samples were centrifuged for 10 min at 12000 rpm prior to gel filtration analysis. The y-axis was normalized to 100 for the 300 mM NaCl trace, and the remaining traces were scaled to this axis to illustrate the loss in intensity caused by precipitation of the protein at low NaCl concentrations. Apparent relative molecular weights of peaks *f*, *g*, and *h* are 190, 130, and 80 kDa, respectively (see Table 1). (D) SDS-PAGE of the total protein (T) and supernatant (S) of the 500 and 50 mM NaCl samples in panel C showing the disappearance of protein in the supernatant fraction of the 50 mM NaCl sample.

s-Mgm1p in the major peak is dynamic and contains a mixture of low-order oligomers that are quickly interconverting. Overall, our gel filtration and cross-linking data suggest s-Mgm1p is able to form low-order oligomers at high salt concentrations. During the initial characterization of

Table 1: Apparent Relative Molecular Weights of s-Mgm1p Gel Filtration Peaks in Figures 1 and 2

peak	apparent relative molecular weight, M_r (kDa)	peak	apparent relative molecular weight, M_r (kDa)
a	390	e	170
b	250	f	190
c	220	g	130
d	200	h	80

s-Mgm1p, we observed the intensity of the minor peak was related to the addition of DTT. We therefore investigated this possibility further.

The Oligomeric State of s-Mgm1p Is Altered by DTT. s-Mgm1p contains seven cysteines, indicating the possibility that each monomer contains at least one free thiol available for intermolecular disulfide bond formation. We investigated the effect of the reducing agent DTT on the oligomeric state of s-Mgm1p by gel filtration chromatography and found the intensity of the minor peak to be reduced when DTT was present (Figure 3B and Table 1). In the absence of DTT, the minor peak is approximately equal in intensity to the major peak; with DTT present, the minor peak is reduced to approximately one-tenth the intensity of the major peak. These results indicate that the oligomer observed as the minor peak is probably a result of an intermolecular disulfide bonding, explaining why the elution volume of this peak is unaffected by protein concentration. Since it has been previously reported that DTT is required for dynamin 1 stability and activity (24), we decided to conduct our studies under reducing conditions and focus on the major peak which is the dominant oligomeric form of s-Mgm1p under these conditions.

The Oligomeric State of s-Mgm1p Is Dependent on the Concentration of NaCl. Oligomerization into rings and high-molecular weight helices in low-salt buffers (<150 mM) is a hallmark of dynamin proteins (5). We therefore tested the effect of salt concentration on s-Mgm1p. Dilution into 150 and 50 mM NaCl buffer resulted in the immediate formation of visible precipitate. The diluted samples were allowed to equilibrate for 24 h at 4 °C and were centrifuged for 10 min at 12000 rpm before analysis. The supernatant collected was analyzed by gel filtration on a Superdex 200 column (Figure 3C and Table 1), and the supernatants (S) and uncentrifuged solutions (T) were visualized by SDS–PAGE (Figure 3D). At 500 and 300 mM NaCl, the protein remained in solution after centrifugation and eluted as a peak with apparent relative molecular weights of ~170 and ~190 kDa, respectively. At 150 mM NaCl, and more pronounced at 50 mM NaCl, the majority of the protein precipitated out of solution as indicated by the disappearance of the 86 kDa band in the supernatant lane of the SDS–PAGE gel, and the marked decrease in intensity of peaks g and h in the gel filtration chromatograms. Analysis of the precipitate formed at low salt concentrations by transmission electron microscopy revealed the presence of disordered aggregates (data not shown). These results indicate that lowering the salt concentration in this manner is not a suitable method for inducing the formation of high-molecular weight complexes of s-Mgm1p.

Determination of GTPase Activity for s-Mgm1p Gel Filtration Fractions. Hallmarks of classical dynamins include a large GTPase domain consisting of ~300 amino acids, low

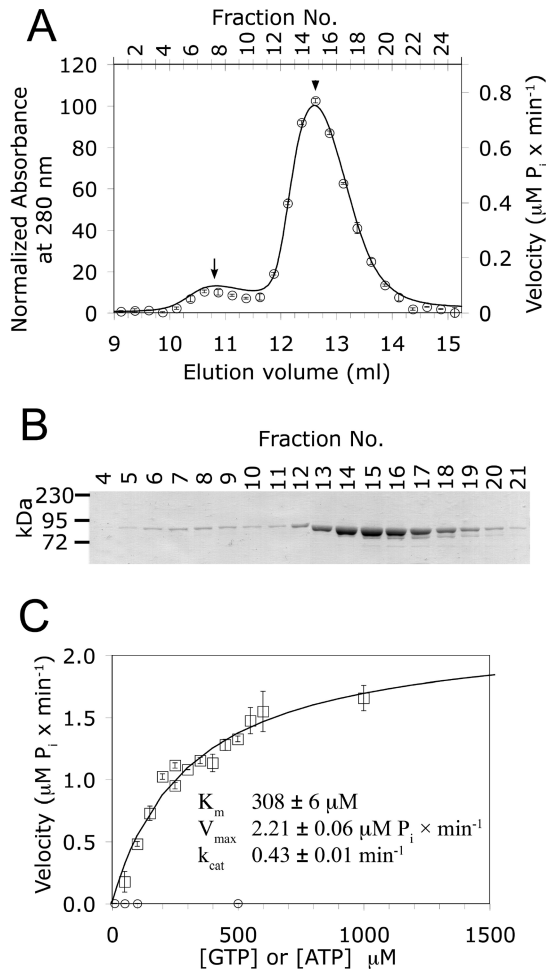


FIGURE 4: GTPase activity of s-Mgm1p. (A) Rate of GTP hydrolysis (\circ , $\mu\text{M P}_i \text{ min}^{-1}$) for minor peak (arrow) and major peak (arrowhead) gel filtration fractions superimposed on the gel filtration chromatogram (black line) showing the rate of hydrolysis is proportional to protein concentration. The average activity of all the fractions, obtained by dividing the amount of inorganic phosphate produced per minute by the protein concentration of each fraction, is $0.263 \pm 0.23 \text{ min}^{-1}$. (B) SDS–PAGE gel of fractions in panel A. (C) Steady-state kinetics of major peak s-Mgm1p with GTP (\square) and ATP (\circ) fit to the Michaelis–Menten equation for enzyme kinetics (black line).

affinity for GTP and GDP, and oligomerization-dependent GTPase activity (5). The predicted GTPase domain of s-Mgm1p contains the four GTP-binding motifs responsible for nucleotide binding and hydrolysis; we therefore tested whether recombinant s-Mgm1p is able to hydrolyze GTP. Initially, we wanted to determine whether GTPase activity coincided with the peaks obtained by gel filtration chromatography. We assayed the ability of the two different oligomeric forms of s-Mgm1p to hydrolyze GTP in 500 mM NaCl buffer (Figure 4A,B) (24). In Figure 4A, the rate of inorganic phosphate produced by each fraction is superimposed on the gel filtration chromatogram. This illustrates the coincidence of the rate of hydrolysis with protein concentration (monitored by absorbance at 280 nm) and confirms that the observed GTPase hydrolysis activity is due to s-Mgm1p. Gel filtration fractions representing the minor and major peaks were all found to have similar activity in the range of $0.263 \pm 0.023 \text{ min}^{-1}$. This indicates that hydrolysis activity is independent of low-order oligomeric state, and cooperation with respect to protein concentration is not observed under

these conditions. Therefore, it is reasonable to conclude that these values represent the basal unstimulated GTPase activity of s-Mgm1p given that the assay was performed at high salt concentrations, there is no difference in the activity of the two low-order oligomeric forms, and the activity values obtained are within the range of dynamin 1 basal activity ($0.1\text{--}2\text{ min}^{-1}$) (24) and 1–3 orders of magnitude lower than stimulated dynamin activity ($5\text{--}258\text{ min}^{-1}$) (5). Together, these data directly demonstrate that s-Mgm1p can hydrolyze GTP.

Determination of Steady-State Kinetics for s-Mgm1p in 500 mM NaCl. We also determined the steady-state kinetics of s-Mgm1p in 500 mM NaCl (Figure 4C). Major peak fractions were pooled, and activity was assayed at different GTP concentrations. This analysis revealed that GTP binding is within the range observed for other dynamins with a K_m of $308 \pm 6\text{ }\mu\text{M}$ (5). The value for k_{cat} is $0.43 \pm 0.01\text{ min}^{-1}$, which is within the range of basal activities previously reported for dynamin ($\sim 0.1\text{--}2\text{ min}^{-1}$) (24) and approximately 1–3 orders of magnitude lower than the stimulated turnover numbers. The high K_m is characteristic of dynamin mechanoenzymes, which have a low affinity for GTP and GDP compared to regulatory GTPases (5). As a control for nucleotide specificity, we also tested the ability of s-Mgm1p to hydrolyze ATP and could not detect any hydrolysis activity with this substrate at concentrations up to 0.5 mM (Figure 4C).

Determination of Basal GTPase Activity for s-Mgm1p Mutants in the GTPase Domain. Previous work has shown that mutations within the GTPase and GED domains of Mgm1p result in a loss of wild-type mitochondrial morphology in *Saccharomyces cerevisiae* (7). Sequence analysis of the GTPase superfamily reveals four highly conserved GTP-binding motifs are present in all GTP binding proteins. In particular, studies have shown that conserved residues in the G1 motif (GxxxxGKS/T) are involved in the coordination of phosphates and that the threonine in the G2 motif is the residue responsible for catalysis (Figure 5A). In vivo characterization of Mgm1p alanine point mutations of S224 in G1 and T244 in G2 showed that S224A and T244A could not complement Δmgm1 defects (7). The GED of dynamin proteins is known to be important for oligomerization and oligomerization-dependent GTPase activity (5). Arginine and lysine residues in this region of Mgm1p were characterized in vivo by being mutated to alanine, and it was found that R824A and K854A had effects on mitochondrial morphology, with the effects of K854A being more severe (7).

To improve our understanding of the roles of the different domains of Mgm1p, we expressed and purified S224A, T244A, and K854A mutants as described for wild-type s-Mgm1p (Figure 5). The mutants have CD spectra and thermal denaturation profiles comparable to those of wild-type s-Mgm1p, indicating the proteins adopt the same fold as the wild-type protein (Figure 5B,C,F,G,J,K). Gel filtration chromatography analysis indicates the mutants have profiles similar to those of wild-type s-Mgm1p, showing a minor peak (arrow) and a concentration-dependent major peak (arrowhead) (Figure 5D,H,L). Of note is the fact that the intensity of the minor peak for the K854A mutant is much lower in comparison to those of WT and the other mutants analyzed, which is consistent with a defect in self-assembly. Cross-linking of the major peak for each mutant reveals the

presence of trimers and higher-order oligomers similar to what is observed for the wild-type (Figure 5E,I,M). To improve our understanding of the effects of these mutations, we analyzed the GTP hydrolysis activity of the two different oligomeric forms of each mutant (Table 2). The mutant in G1 of the GTPase domain, S224A, showed a 3-fold reduced activity for the minor peak and a complete abolishment of activity for the major peak compared to wild-type s-Mgm1p. The threonine to alanine mutation, T244A, which abolishes the predicted catalytically active residue, shows a 40-fold reduction in activity for the minor peak and a complete abolishment of activity for the major peak. The activity of the GED domain mutant K854A could not be quantified for the minor peak because this peak was much less intense in comparison to those of all the other mutants. The major peak exhibited activity comparable to that of wild-type s-Mgm1p, which is consistent with this mutant having a functional GTPase domain, and further substantiating that the activity measured for wild-type Mgm1p is that of the unassembled protein since this mutant is presumed to have an oligomerization defect. These results verify that the GTPase activity observed for wild-type Mgm1p is due to an active GTPase domain and confirm in vivo defects are a result of GTP binding or hydrolysis and oligomerization.

s-Mgm1p Binds to Negatively Charged Lipids in Vitro. Conventional sequence analysis tools do not detect the presence of a PH domain in Mgm1p; however, other DRPs such as ADL2, Dnm1, and MxA, which also do not contain PH domains, are known to bind negatively charged lipids. A lipid-binding domain may not be necessary for Mgm1p targeting since it has been documented that the protein associates with the outer membrane via interactions with Fzo1p and Ugo1p (3, 7) and with the inner membrane via a hydrophobic segment (6). To probe whether s-Mgm1p interacts with lipids, we tested a series of lipids found in the mitochondrial membrane or documented to bind to PH domains using a lipid overlay assay (Figure 6A). Interestingly, we found that s-Mgm1p interacts with the negatively charged lipids cardiolipin, phosphatidic acid, phosphatidylserine, and phosphatidylinositol 3,5-bisphosphate, but not with other negatively charged lipids such as phosphatidylinositol, other phosphatidylinositol phosphates, and phosphatidylglycerol, a precursor of cardiolipin. s-Mgm1p does not interact with the most abundant components of the mitochondrial inner and outer membranes, the zwitterionic phospholipids phosphatidylcholine and phosphatidylethanolamine. An alignment of 22 fungal sequences homologous to Mgm1p reveals that there is conservation of lysines and arginines in the region of the protein between the middle domain and GED that could mediate the interaction with negative lipids (Figure 6B). To determine whether residues in this region are important for lipid interaction, we mutagenized conserved lysines and arginines in the predicted PH domain of Mgm1p. We successfully purified mutants K544A, K566A, K637A, K699A, K702A, K745A, R783A, and K795A and analyzed them using the lipid overlay assay. Of the mutants we tested, we found that K795A was not able to bind phosphatidylserine and had a weaker affinity for cardiolipin and phosphatidic acid in comparison to wild-type Mgm1p and the remaining mutants that were tested (Figure 6C). We also identified three mutants (K544A, K566A, and K724A) that were impaired with respect to

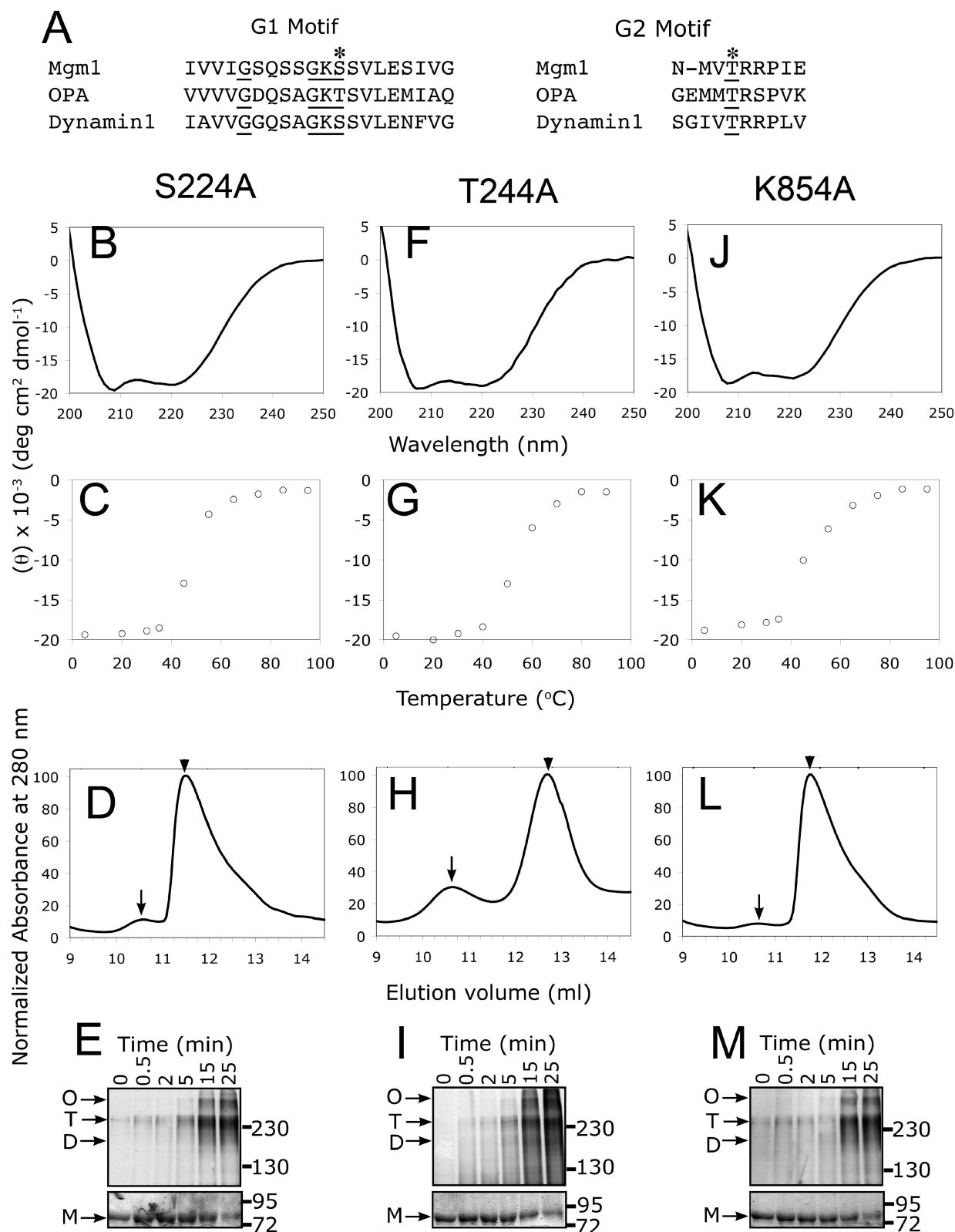


FIGURE 5: s-Mgmlp mutants in the GTPase domain and GED. (A) Sequence alignment of the G1 and G2 motifs from the GTPase domain showing Mgmlp, OPA, and dynamin 1: conserved residues (underlined) and residues mutated to alanine (asterisks). (B, F, and J) CD spectra of S224A, T244A, and K854A, respectively, expressed as mean residue ellipticity, at 5 °C. (C, G, and K) Thermal denaturation of S224A, T244A, and K854A, respectively, monitored by circular dichroism at 208 nm. CD experiments were performed with 2.5 μ M S224A, 0.7 μ M T244A, and 2.9 μ M K854A. (D, H, and L) Representative gel filtration chromatograms for S224A, T244A, and K854A, respectively, depicting the presence of a minor peak (arrow) and major peak (arrowhead) and showing a concentration-dependent shift in the major peak: 25 mg/mL S224A, 4.5 mg/mL T244A, and 14.6 mg/mL K854A. The y-axis was scaled to 100 for each mutant. (E, I, and M) Cross-linking of the major peaks of S224A, T244A, and K854A, respectively. Bottom panels are Coomassie Blue-stained gels showing the disappearance of monomer (M). Top panels are silver-stained gels showing the predominant formation of trimers (T), larger oligomers (O), and dimers (D). All cross-linking was performed with 0.6 mg/mL protein and 0.025% glutaraldehyde at 4 °C.

Table 2: GTPase Activity for the Minor and Major Peaks of Wild-Type and Mutant s-Mgm1p

	activity (min ⁻¹)	
	minor peak ^a	major peak ^a
wild-type	0.274 ± 0.036	0.265 ± 0.004
S224A	0.083 ± 0.015	0.001 ± 0.001
T244A	0.007 ± 0.001	0.001 ± 0.001
K854A	n/a ^b	0.354 ± 0.014

^a Activity values for each protein were determined on equivalent gel filtration fractions of the minor and major peaks. ^b Fractions did not contain quantifiable amounts of protein.

phosphatidic acid binding (see the Supporting Information). These results suggest that s-Mgm1p contains a lipid-binding domain that is specific for negatively charged phospholipids found in mitochondrial membranes.

DISCUSSION

Molecules involved in mitochondrial fusion are evolutionarily conserved from yeast to humans and have direct human health consequences (1, 2, 8). In particular, mutations in the human homologue of Mgm1p, OPA1, are responsible for autosomal dominant optic atrophy, a neuropathy characterized by optic nerve degeneration and onset in the first decade of life (2, 28). Several lines of evidence have demonstrated that Mgm1p is responsible for mitochondrial inner membrane fusion and cristae structure maintenance, but its molecular role in this process and mode of action have remained elusive.

In this paper, we directly demonstrate that purified s-Mgm1p is able to self-associate in vitro indicating this protein functions in a manner similar to that of dynamin and supporting the yeast mitochondria fusion experiments that suggest oligomerization is required to mediate fusion and cristae structure maintenance (18). We found that the predominant form of s-Mgm1p in nonassembly conditions is a dynamic, concentration-dependent low-order oligomeric mixture. We observe a protein concentration-dependent shift in gel filtration peaks reflecting a progression to higher-order oligomers with an increase in protein concentration (Figure 3A). In addition, peak broadening and asymmetry in Figure 3A and the inability to resolve discrete oligomeric species both indicate that s-Mgm1p self-association is rapid and reversible (26). Together, our characterization of s-Mgm1p oligomeric state by gel filtration and chemical cross-linking indicate that the protein forms low-order dynamic oligomers at high salt concentrations. To fully characterize the oligomeric behavior of s-Mgm1p and determine oligomer stoichiometries and dissociation constants, a comprehensive analytical ultracentrifugation study as a function of protein concentration would be required for this complex system. Overall, the dynamic nature of Mgm1p intermolecular interactions is consistent with an in vivo role in inner membrane fusion and cristae maintenance that requires the formation of different length oligomers that are able to reversibly associate.

We also investigated the behavior of s-Mgm1p under low-ionic strength conditions, but our results indicate that although s-Mgm1p forms high-molecular weight assemblies under these conditions, they are likely nonspecific (Figure 3C and Table 1). We determined that both the oligomeric mixture of s-Mgm1p containing the minor and major peaks,

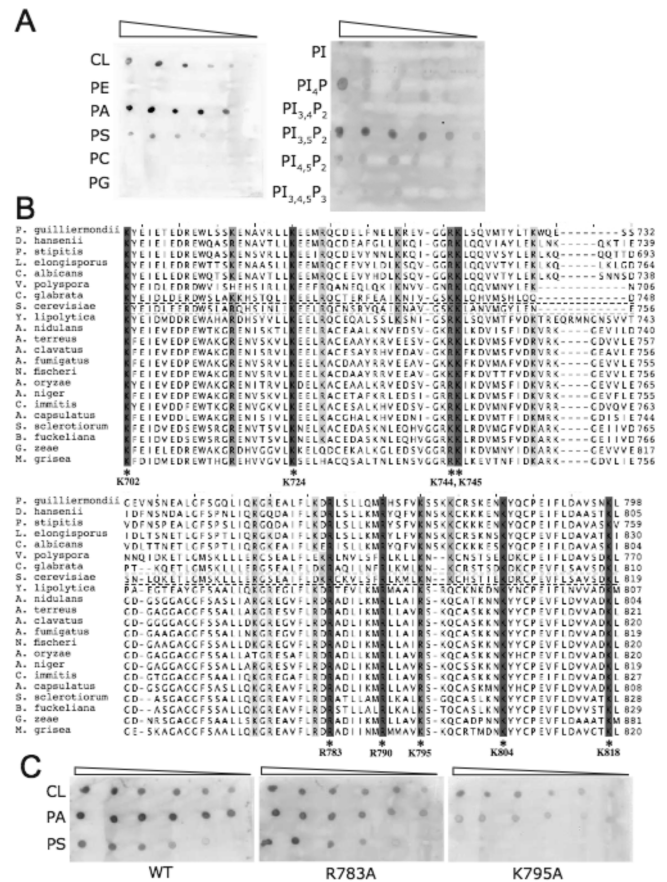


FIGURE 6: s-Mgm1p phospholipid binding. (A) Lipid overlay assay. Serial dilutions (500, 250, 125, 62.5, 31.2, and 15 pmol) of the indicated phospholipids were spotted onto a nitrocellulose membrane and incubated with 10 nM s-Mgm1p-His₆. Binding was detected with anti-His₆ antibodies. Abbreviations: CL, cardiolipin; PA, phosphatidic acid; PS, phosphatidylserine; PE, phosphatidylethanolamine; PC, phosphatidylcholine; PG, phosphatidylglycerol; PI, phosphatidylinositol; PI₄P, phosphatidylinositol 4-phosphate; PI_{3,4}P, phosphatidylinositol 3,4-bisphosphate; PI_{3,5}P, phosphatidylinositol 3,5-bisphosphate; PI_{4,5}P, phosphatidylinositol 4,5-bisphosphate; PI_{3,4,5}P, phosphatidylinositol 3,4,5-triphosphate. (B) Alignment of the putative lipid-binding domain found between the middle domain and the GED of Mgm1p with a variety of fungus homologues identified using BLAST (27). In this alignment, lysine and arginine residues that are 100% conserved are colored dark gray (asterisks) and lysines and arginines that are >30% conserved are identified by increasing levels of darkness. Species and database entries: *Pichia guilliermondii*, gil190347643; *Debaryomyces hanseni*, gil50427515; *Pichia stipitis*, gil150951259; *Lodderomyces elongisporus*, gil149237060; *Candida albicans*, gil68470872; *Vanderwaltozyma polyspora*, gil156843934; *Candida glabrata*, gil50292919; *S. cerevisiae*, gil190407521 Mgm1p; *Yarrowia lipolytica*, gil50555692; *Aspergillus nidulans*, gil67517829; *Aspergillus terreus*, gil115491707; *Aspergillus clavatus*, gil121701617; *Aspergillus fumigatus*, gil70995616; *Neosartorya fischeri*, gil119495564; *Aspergillus oryzae*, gil169768832; *Aspergillus niger*, gil145239791; *Coccidioides immitis*, gil119174070; *Ajellomyces capsulatus*, gil154281121; *Sclerotinia sclerotiorum*, gil156041160; *Botryotinia fuckeliana*, gil154290236; *Gibberella zeae*, gil46126151; *Magnaporthe grisea*, gil145606220. (C) Lipid overlay assay using the same dilution series as in panel A and incubated with 10 nM wild-type, R783A, and K795A s-Mgm1p-His₆.

and the major peak alone, rapidly form very high-molecular weight aggregates when placed in low salt that can be readily sedimented at low centrifugation speeds. Moreover, gel filtration analysis of the supernatants of these samples does not indicate the presence of any species with a molecular weight higher than that of the minor peak, suggesting that

species of intermediate molecular weight are not present at low salt concentrations. These findings indicate that rapidly lowering the ionic strength does not induce the formation of ordered polymers that represent functionally relevant assemblies as documented for other members of the dynamin superfamily and is not a suitable protocol for promoting Mgm1p self-association. The methodology for inducing the self-assembly of s-Mgm1p low-order oligomers into higher-order polymers will be required before these species can be studied by electron microscopy. These studies would allow for further insight into the complex mechanism of Mgm1p-mediated membrane fusion.

Two key features distinguish the GTPase domain of dynamin proteins. The first is a low affinity for GTP and GDP in comparison to Ras-like GTPase, which abolishes the need for nucleotide exchange factors but implies that dynamins require constitutive loading of GTP under physiological conditions (5, 29). The second is a stimulated rate of GTP hydrolysis for the ordered, high-molecular weight oligomers. This is likely a result of the intermolecular interaction between the GED, thought to be analogous to the GTPase activating proteins of Ras-like GTPases in stimulating activity, and the GTPase, middle domain, and GED of adjacent Mgm1p molecules. Studies in yeast cells and of purified yeast mitochondria indicate that a functional Mgm1p GTPase domain is required for correct mitochondrial morphology and successful inner membrane fusion (7, 18, 19, 30). It has also been determined through an in vitro mitochondrial fusion assay that Mgm1p-mediated inner membrane fusion necessitates high levels of GTP (0.5 mM) and an inner membrane potential (17).

Here we show that purified Mgm1p has basal GTP hydrolysis activity. GTP hydrolysis assessed under nonassembly conditions showed no significant difference in the activities of the two oligomeric forms of Mgm1p detected by gel filtration (Figure 4A,B). Furthermore, consistent with in vitro mitochondrial fusion experiments showing high levels of exogenous GTP (0.5 mM) are required for inner membrane fusion, kinetic analysis of s-Mgm1p revealed that it has a weak affinity for GTP with a K_m equal to $308 \pm 6 \mu\text{M}$. This value is within the range documented for other dynamin proteins which varies from 8–15 μM for mammalian dynamin 1 to 470 μM for *Homo sapiens* GBP1 (5) and is a strong indicator that Mgm1p is the enzyme carrying out GTP hydrolysis during the in vitro mitochondrial fusion assay. The basal turnover number for s-Mgm1p is $0.43 \pm 0.01 \text{ min}^{-1}$ and falls within the reported range of dynamin 1 basal activities ($0.1\text{--}2 \text{ min}^{-1}$) (24). Rates of stimulated dynamin 1 activity are as high as 260 min^{-1} ; however, we expect that Mgm1p should have a slower stimulated rate of hydrolysis since its function is not membrane scission as it is for dynamin 1. Indeed, it has been proposed that a slower rate of GTP hydrolysis could lead to the deformation of membranes into tubular projections (tubulation), indicating a possible mode of action for Mgm1p in bringing two membranes in close apposition and/or inducing membrane curvature which facilitates fusion (5). The kinetic data shown here also indicate that Mgm1p functions as a mechanoenzyme rather than a switch GTPase, the latter characterized by subnanomolar GTP binding and slow intrinsic hydrolysis. Together, our data clearly demonstrate that Mgm1p can

specifically hydrolyze GTP in a manner consistent with its prescribed role in inner membrane fusion.

The four canonical GTP-binding motifs are highly conserved in Mgm1p. The G1 motif contains key residues responsible for phosphate coordination, while the G2 motif contains the catalytic threonine (Figure 5A). Alanine mutations of serine 224 of the G1 motif and threonine 244 of the G2 motif were shown to exhibit aberrant mitochondrial morphology, indicating a defect in mitochondrial fusion (7). In addition, mutations eliminating positively charged lysine and arginine residues in the GED domain were shown to interfere with self-assembly. Wong and colleagues mutated all the lysines and arginines in the GED domain of Mgm1p and showed that R824A and K854A produced aberrant mitochondria. We purified and characterized S224A, T244A, and K854A and demonstrated that these mutants have CD spectra identical to those of wild-type protein and a chemical cross-linking and gel filtration profile similar to that of wild-type s-Mgm1p, the latter showing two populations of oligomeric proteins forming a minor (arrow) and major peak (arrowhead) (Figure 5D,H,L). The differences in elution volumes among the major peaks of the various mutants are due to different protein concentrations injected onto the column and demonstrate the concentration dependence and reversibility of the oligomers in this peak. As with wild-type s-Mgm1p, the elution volume of the minor peak remains constant for all the mutants and concentrations assayed. Interestingly, the ability of K854A to form minor peak oligomers was greatly reduced compared to that of the wild-type and the other mutants, indicating a defect in self-assembly (Figure 5L, arrow). However, K854A was still able to self-assemble into basal (major peak) oligomers and hydrolyze GTP at the same rate as the wild-type (Table 2). A mutation in the same region of the GED of dynamin 1, K694A, also showed a decreased propensity for self-assembly, a lower assembly-stimulated rate of hydrolysis, and basal hydrolysis similar to that of the wild-type (31). These observations indicate that K854 is not involved in the intermolecular interactions that form the basic oligomer of Mgm1p but could be important in the formation of higher-order structures. This suggests that the defect observed in K854A cells results from the inability of Mgm1p to self-assemble since the protein is still hydrolytically active and further supports the idea that the function of Mgm1p is oligomerization-dependent. We also directly show that both S224A and T244A mutants lack the ability to hydrolyze GTP, demonstrating that the defect observed in cells harboring these mutations are indeed due to impaired GTP turnover (Table 2). Taken together, our data provide direct evidence that supports the hypothesis that Mgm1p acts in a GTP-dependent manner and requires the ability to hydrolyze GTP and self-associate to mediate mitochondrial inner membrane fusion and cristae structure maintenance.

Previous studies have shown that Mgm1p is found in the inter membrane space peripherally associated with the inner membrane (7, 19) and also associates with the outer membrane (30, 32) probably as a result of interacting with the outer membrane fusion components Fzo1p and Ugo1p. l-Mgm1p is presumed to be tethered to the inner membrane via a hydrophobic patch containing the Rbd1p cleavage site important for the formation of s-Mgm1p (6). These findings, along with the fact that conventional sequence analysis tools

do not detect the presence of a PH domain in Mgm1p, might indicate that membrane targeting of this protein is probably achieved via protein–protein interactions on the outer and inner membranes. Interestingly, however, other DRPs such as ADL2, Dnm1, and MxA, which also lack PH domains, are known to interact with negatively charged lipids, possibly because the inherent curvature of the assembled polymers can associate with lipid bilayers (9, 10). To determine whether s-Mgm1p interacts with lipids, we conducted a protein lipid overlay assay (25) and found that s-Mgm1p associates specifically with the negatively charged phospholipids, cardiolipin, phosphatidic acid, phosphatidylserine, and phosphatidylinositol 3,4-bisphosphate. s-Mgm1p does not interact with the negative phospholipids phosphatidylglycerol, phosphatidylinositol, and phosphatidylinositol phosphates or with the neutral and most abundant phospholipids in the mitochondrial membrane, phosphatidylcholine and phosphatidylethanolamine. To further characterize lipid binding, we mutated several conserved lysine and arginine residues in the predicted PH domain of Mgm1p. We found that K795A completely abrogates phosphatidylserine binding and weakens binding to cardiolipin and phosphatidic acid (Figure 6C). Furthermore, we also identified three mutants (K544A, K566A, and K724A) that show decreased affinity for phosphatidic acid (Figure S1 of the Supporting Information). Although phosphatidic acid is a minor component of mitochondrial membranes (33), this phospholipid has been implicated in plasma membrane fusion events likely through its ability to induce membrane curvature (34, 35). The identification of lysine residues mediating interactions with specific phospholipids indicates that lipid binding is a selective and therefore physiologically relevant phenomenon. Together, our data indicate the presence of a potential novel lipid-binding module in Mgm1p that could provide key insight into the role of this protein in inner membrane fusion and cristae maintenance. Furthermore, our assay suggests it is the interaction with phospholipid head groups and not the curvature of the assembled form of s-Mgm1p that mediates protein–lipid interactions. This could suggest the presence of an unidentified or highly divergent lipid-binding module in other DRPs with lipid binding properties such as ADL2, Dnm1, and MxA. We are currently working toward identifying other residues involved in lipid binding and understanding the functional significance of lipid binding in vitro and in yeast cells.

Interestingly, missense mutations causing dominant optic atrophy in humans have been identified in both the GTPase domain and GED of OPA1, suggesting the mechanism of action of Mgm1p in mitochondrial fusion and cristae maintenance is conserved across eukaryotes. Our biochemical studies establish the importance of the GTPase domain and GED to the cellular function of this protein and highlight the relevance of the mutations linked to human disease.

SUPPORTING INFORMATION AVAILABLE

Lipid overlay assay of wild-type s-Mgm1p and phosphatidic acid binding mutants. This material is available free of charge via the Internet at <http://pubs.acs.org>.

REFERENCES

- Hoppins, S., Lackner, L., and Nunnari, J. (2007) The machines that divide and fuse mitochondria. *Annu. Rev. Biochem.* 76, 751–780.
- Chen, H., and Chan, D. C. (2005) Emerging functions of mammalian mitochondrial fusion and fission. *Hum. Mol. Genet.* 14 (Spec. No. 2), R283–R289.
- Sesaki, H., and Jensen, R. E. (2004) Ugo1p links the Fzo1p and Mgm1p GTPases for mitochondrial fusion. *J. Biol. Chem.* 279, 28298–28303.
- Okamoto, K., and Shaw, J. M. (2005) Mitochondrial morphology and dynamics in yeast and multicellular eukaryotes. *Annu. Rev. Genet.* 39, 503–536.
- Praefcke, G. J., and McMahon, H. T. (2004) The dynamin superfamily: Universal membrane tubulation and fission molecules? *Nat. Rev. Mol. Cell Biol.* 5, 133–147.
- Herlan, M., Bornhøvd, C., Hell, K., Neupert, W., and Reichert, A. S. (2004) Alternative topogenesis of Mgm1 and mitochondrial morphology depend on ATP and a functional import motor. *J. Cell Biol.* 165, 167–173.
- Wong, E. D., Wagner, J. A., Scott, S. V., Okreglak, V., Holewinski, T. J., Cassidy-Stone, A., and Nunnari, J. (2003) The intramitochondrial dynamin-related GTPase, Mgm1p, is a component of a protein complex that mediates mitochondrial fusion. *J. Cell Biol.* 160, 303–311.
- Zhang, Y., and Chan, D. C. (2007) New insights into mitochondrial fusion. *FEBS Lett.* 581, 2168–2173.
- Mears, J. A., and Hinshaw, J. E. (2008) Visualization of dynamins. *Methods Cell Biol.* 88, 237–256.
- Kim, Y. W., Park, D. S., Park, S. C., Kim, S. H., Cheong, G. W., and Hwang, I. (2001) Arabidopsis dynamin-like 2 that binds specifically to phosphatidylinositol 4-phosphate assembles into a high-molecular weight complex in vivo and in vitro. *Plant Physiol.* 127, 1243–1255.
- Melen, K., Ronni, T., Broni, B., Krug, R. M., von Bonsdorff, C. H., and Julkunen, I. (1992) Interferon-induced Mx proteins form oligomers and contain a putative leucine zipper. *J. Biol. Chem.* 267, 25898–25907.
- Hinshaw, J. E., and Schmid, S. L. (1995) Dynamin self-assembles into rings suggesting a mechanism for coated vesicle budding. *Nature* 374, 190–192.
- Shin, H. W., Takatsu, H., Mukai, H., Munekata, E., Murakami, K., and Nakayama, K. (1999) Intermolecular and interdomain interactions of a dynamin-related GTP-binding protein, Dnm1p/Vps1p-like protein. *J. Biol. Chem.* 274, 2780–2785.
- Eccleston, J. F., Binns, D. D., Davis, C. T., Albanesi, J. P., and Jameson, D. M. (2002) Oligomerization and kinetic mechanism of the dynamin GTPase. *Eur. Biophys. J.* 31, 275–282.
- Herlan, M., Vogel, F., Bornhøvd, C., Neupert, W., and Reichert, A. S. (2003) Processing of Mgm1 by the rhomboid-type protease Pcp1 is required for maintenance of mitochondrial morphology and of mitochondrial DNA. *J. Biol. Chem.* 278, 27781–27788.
- McQuibban, G. A., Saurya, S., and Freeman, M. (2003) Mitochondrial membrane remodelling regulated by a conserved rhomboid protease. *Nature* 423, 537–541.
- Meeusen, S., McCaffery, J. M., and Nunnari, J. (2004) Mitochondrial fusion intermediates revealed in vitro. *Science* 305, 1747–1752.
- Meeusen, S., DeVay, R., Block, J., Cassidy-Stone, A., Wayson, S., McCaffery, J. M., and Nunnari, J. (2006) Mitochondrial inner-membrane fusion and crista maintenance requires the dynamin-related GTPase Mgm1. *Cell* 127, 383–395.
- Wong, E. D., Wagner, J. A., Gorsich, S. W., McCaffery, J. M., Shaw, J. M., and Nunnari, J. (2000) The dynamin-related GTPase, Mgm1p, is an intermembrane space protein required for maintenance of fusion competent mitochondria. *J. Cell Biol.* 151, 341–352.
- Vogel, F., Bornhøvd, C., Neupert, W., and Reichert, A. S. (2006) Dynamic subcompartmentalization of the mitochondrial inner membrane. *J. Cell Biol.* 175, 237–247.
- Amutha, B., Gordon, D. M., Gu, Y., and Pain, D. (2004) A novel role of Mgm1p, a dynamin-related GTPase, in ATP synthase assembly and cristae formation/maintenance. *Biochem. J.* 381, 19–23.
- Frezza, C., Cipolat, S., Martins de Brito, O., Micaroni, M., Beznoussenko, G. V., Rudka, T., Bartoli, D., Polishuck, R. S., Danial, N. N., De Strooper, B., and Scorrano, L. (2006) OPA1 controls apoptotic cristae remodeling independently from mitochondrial fusion. *Cell* 126, 177–189.
- Olichon, A., Baricault, L., Gas, N., Guillou, E., Valette, A., Belenguer, P., and Lenaers, G. (2003) Loss of OPA1 perturbs

- the mitochondrial inner membrane structure and integrity, leading to cytochrome c release and apoptosis. *J. Biol. Chem.* 278, 7743–7746.
24. Leonard, M., Song, B. D., Ramachandran, R., and Schmid, S. L. (2005) Robust colorimetric assays for dynamin's basal and stimulated GTPase activities. *Methods Enzymol.* 404, 490–503.
 25. Dowler, S., Kular, G., and Alessi, D. R. (2002) Protein lipid overlay assay. *Sci. STKE* 2002, PL6.
 26. Winzor, D. J. (2003) Analytical exclusion chromatography. *J. Biochem. Biophys. Methods* 56, 15–52.
 27. Altschul, S. F., and Lipman, D. J. (1990) Protein database searches for multiple alignments. *Proc. Natl. Acad. Sci. U.S.A.* 87, 5509–5513.
 28. Alexander, C., Votruba, M., Pesch, U. E., Thiselton, D. L., Mayer, S., Moore, A., Rodriguez, M., Kellner, U., Leo-Kottler, B., Auburger, G., Bhattacharya, S. S., and Wissinger, B. (2000) OPA1, encoding a dynamin-related GTPase, is mutated in autosomal dominant optic atrophy linked to chromosome 3q28. *Nat. Genet.* 26, 211–215.
 29. Krishnan, K. S., Rikhy, R., Rao, S., Shivalkar, M., Mosko, M., Narayanan, R., Etter, P., Estes, P. S., and Ramaswami, M. (2001) Nucleoside diphosphate kinase, a source of GTP, is required for dynamin-dependent synaptic vesicle recycling. *Neuron* 30, 197–210.
 30. Sesaki, H., Southard, S. M., Hobbs, A. E., and Jensen, R. E. (2003) Cells lacking Pcp1p/Ugo2p, a rhomboid-like protease required for Mgm1p processing, lose mtDNA and mitochondrial structure in a Dnm1p-dependent manner, but remain competent for mitochondrial fusion. *Biochem. Biophys. Res. Commun.* 308, 276–283.
 31. Sever, S., Muhlberg, A. B., and Schmid, S. L. (1999) Impairment of dynamin's GAP domain stimulates receptor-mediated endocytosis. *Nature* 398, 481–486.
 32. Shepard, K. A., and Yaffe, M. P. (1999) The yeast dynamin-like protein, Mgm1p, functions on the mitochondrial outer membrane to mediate mitochondrial inheritance. *J. Cell Biol.* 144, 711–720.
 33. Zinser, E., Sperka-Gottlieb, C. D., Fasch, E. V., Kohlwein, S. D., Paltauf, F., and Daum, G. (1991) Phospholipid synthesis and lipid composition of subcellular membranes in the unicellular eukaryote *Saccharomyces cerevisiae*. *J. Bacteriol.* 173, 2026–2034.
 34. Zeniou-Meyer, M., Zabari, N., Ashery, U., Chasserot-Golaz, S., Haeberle, A. M., Demais, V., Bailly, Y., Gottfried, I., Nakanishi, H., Neiman, A. M., Du, G., Frohman, M. A., Bader, M. F., and Vitale, N. (2007) Phospholipase D1 production of phosphatidic acid at the plasma membrane promotes exocytosis of large dense-core granules at a late stage. *J. Biol. Chem.* 282, 21746–21757.
 35. Kooijman, E. E., Chupin, V., Fuller, N. L., Kozlov, M. M., de Kruijff, B., Burger, K. N., and Rand, P. R. (2005) Spontaneous curvature of phosphatidic acid and lysophosphatidic acid. *Biochemistry* 44, 2097–2102.

BI801723D